Ecological Informatics 82 (2024) 102679

Contents lists available at ScienceDirect

Ecological Informatics

journal homepage: www.elsevier.com/locate/ecolinf

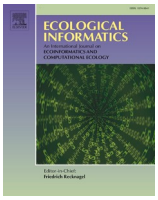

Will artificial intelligence revolutionize aerial surveys? A first large-scale semi-automated survey of African wildlife using oblique imagery and deep learning

Alexandre Delplanque [a,*], Julie Linchant [a], Xavier Vincke [b], Richard Lamprey [c], Jérôme Théau [d,e], Cédric Vermeulen [a], Samuel Foucher [d], Amara Ouattara [f], Roger Kouadio [f], Philippe Lejeune [a]

[a] TERRA Teaching and Research Centre (Forest Is Life), ULiège, Gembloux Agro-Bio Tech, Passage des Déportés 2, Gembloux 5030, Belgium
[b] Aviation Sans Frontières (ASF) Belgique ASBL, Rue Montoyer 1 - Bte 36, Bruxelles B-1000, Belgium
[c] Wildlife Consultant, Midleton, Co. Cork, Ireland
[d] Department of Applied Geomatics, Université de Sherbrooke, 2500 Boulevard de l'Université, Sherbrooke, QC J1K 2R1, Canada
[e] Quebec Centre for Biodiversity Science (QCBS), Stewart Biology, McGill University, Montréal, QC H3A 1B1, Canada
[f] Office Ivoirien des Parcs et Réserves (OIPR), 936J+4F, Abidjan, Côte d'Ivoire

ARTICLE INFO

Keywords:
Wildlife population estimation
Aerial surveys
Deep learning
Biodiversity monitoring
Conservation technology
African savanna

ABSTRACT

Large African mammal populations are traditionally estimated using the systematic reconnaissance flights (SRF) with rear-seat observers (RSOs). The oblique-camera-count (OCC) approach, utilizing digital cameras on aircraft sides, proved to provide more reliable population estimates but incurs high manual processing costs. Addressing the urgent need for efficiency, the research explores whether a semi-automated deep learning (SADL) model coupled with OCC improves wildlife population estimates compared to the SRF-RSO method. The study area was the Comoé National Park, in Ivory Coast, spanning 11,488 km^2 of savannas and open forests. It was surveyed following both SRF-RSO standards and OCC method. Key species included the elephant, western hartebeest, roan antelope, buffalo, kob, waterbuck and warthog. The deep learning model *HerdNet*, priorly pre-trained on images from Uganda, was incorporated in the SADL pipeline to process the 190,686 images. It involved three human verification steps to ensure quality of detections and to avoid overestimating counts. The entire pipeline aims to balance efficiency and human effort in wildlife population estimation. RSO and SADL-OCC approaches were compared using the Jolly II analysis and a verification of 200 random RSO observations. Jolly II analysis revealed SADL-OCC estimates significantly higher for small-sized species (kob, warthog) and comparable for other key species. Counting differences were mainly attributed to vegetation obstruction, RSO observations not found in the images, and suspected RSO counting errors. Human effort in the SADL-OCC approach totaled 111 h, representing a significant time savings compared to a fully manual interpretation. Introducing the SADL approach for aerial surveys in Comoé National Park enabled us to address the OCC's time-intensive image interpretation. Achieving a significant reduction in human workload, our method provided population estimates comparable to or better than SRF-RSO counts. Vegetation obstruction was a key factor explaining differences, highlighting the OCC method's limitation in vegetated areas. Method comparisons emphasized SADL-OCC's advantages in spotting isolated, small and static animals, reducing count variance between sample units. Despite limitations, the SADL-OCC approach offers transformative potential, suggesting a shift towards DL-assisted aerial surveys for increased efficiency and affordability, especially using microlight aircraft and drones in future wildlife monitoring initiatives.

* Corresponding author.
E-mail address: alexandre.delplanque@uliege.be (A. Delplanque).

https://doi.org/10.1016/j.ecoinf.2024.102679
Received 25 December 2023; Received in revised form 6 May 2024; Accepted 7 June 2024
Available online 8 June 2024

1. Introduction

Although biodiversity loss has a significant impact on Earth's ecosystem functions (Cardinale et al., 2012), it is still accelerating following the growth of human population, consumption rates and the continuing pressure humans exert on the biosphere (Ceballos and Ehrlich, 2023). Determining and tracking key-species populations with standardized data collection is seen as critical in the 'essential biodiversity variables' (EBVs) for effective biodiversity assessment and conservation (Jetz et al., 2019). Among the many existing census methods, aerial surveys are still the most economical and quicker way to count large mammals in Africa's large savanna protected areas (PAs) (Norton-Griffiths, 1978).

Counting large terrestrial wildlife species and livestock has traditionally relied on the 'systematic reconnaissance flight' (SRF) method. SRF consists of aircraft flying at low altitude along predefined transects, while rear-seat observers (RSOs) count animals in right and left sample strips defined by markers attached to the aircraft (Grimsdell and Westley, 1981; Norton-Griffiths, 1978). While this technique has been adopted as a standard in African savannas (CITES-MIKE, 2020; Craig, 2012; Norton-Griffiths, 1978; PAEAS, 2014), it suffers from human counting errors as RSOs may under- or overcount large herds, miss species, or lose attention during long flights. Counting animals on sight is challenging. It is often biased by survey factors such as altitude, sample strip width or observer experience (Caughley, 1974; Jachmann, 2001; Norton-Griffiths, 1976), but also by environmental factors such as animal size and color, animal's disturbance caused by an overflying aircraft, group size or vegetation type and density (Griffin et al., 2013; Jachmann, 2002; Wal et al., 2011). To minimize the impact of some of these factors, aerial survey standards for fixed-wing aircraft have been established (CITES-MIKE, 2020; Craig, 2012; PAEAS, 2014). However, the high flight speed (150–190 km/h), essential to ensure the crew's safety at common flying altitude (90–100 m), leaves the observer only a small window of time to scan the terrain and to count animals. This window being estimated at only 5–7 s (Lamprey et al., 2020b), observers may be overloaded in high-density animal environments or tired in low-density ones, which could both lead to biased counts (Norton-Griffiths, 1976). Although not always adopted by practitioners, photographing herds for post-processing is a beneficial practice during aerial surveys, as even experienced observers are unable to accurately count groups of >20 individuals (Norton-Griffiths, 1978). It is even recommended to photograph any group of >10 individuals in the case of multi-species survey (CITES-MIKE, 2020; Norton-Griffiths, 1978). Counts derived from the images are then used to correct in-sight count and provide unbiased estimates.

To compensate for the limits of the SRF method, the oblique-camera-count (OCC) approach has recently been developed and has proved to increase and precise the estimates of large African mammal species in semi-arid environments (Lamprey et al., 2020a, 2020b). The OCC approach is based on digital cameras placed on both right and left sides of the aircraft, replicating the oblique viewing angle of RSOs which is the most suitable for counting animals in areas with vegetation cover (Lamprey et al., 2020b). These cameras are set to acquire images continuously during the SRF. With this method, the work of observers has shifted from in-sight animal counting in the aircraft to image interpretation in the lab. Nevertheless, counting animals in aerial imagery is a time-consuming exercise which may generate considerable costs, making the approach too expensive for a broader use at present (Bröker et al., 2019; Lamprey et al., 2020b). Previous studies showed that interpreters were able to interpret nearly 150 nadir images per hour from a mono-species drone survey in homogeneous Asian open grasslands (Peng et al., 2020) but only 30 oblique images per hour from a multi-species aerial survey in heterogeneous semi-arid African environments where many variables, including vegetation type, are measured (Lamprey et al., 2020b). While being essential for rapidly validating or establishing conservation actions, results from aerial surveys of PAs covering thousands of square kilometers and generating thousands of images can be delayed by several months using the OCC approach due to the slow but necessary manual processing of images.

Recent advances in machine learning have propelled the perspectives of remotely sensed imagery for wildlife conservation (Tuia et al., 2022), and announced good prospects for the automation of image processing from SRF-OCC surveys (Delplanque et al., 2023b; Eikelboom et al., 2019). Deep learning (DL) is a subgroup of machine learning and artificial intelligence (AI) where artificial neural networks are trained to achieve challenging tasks (e.g. detect animals in aerial imagery) through a complex multi-level representation of information learned from a large amounts of data (LeCun et al., 2015). In the last decade, DL has been widely employed to (semi-)automate the detection and counting of multiple terrestrial mammals on aerial imagery acquired in natural and wild environments, through mainly DL-based object detection approaches (Delplanque et al., 2022; Delplanque et al., 2023a; Eikelboom et al., 2019; Kellenberger et al., 2018; Naudé and Joubert, 2019; Peng et al., 2020). However, counting results obtained with these approaches remain biased, principally for rare species, due to the high false positive rate of current DL models and to the limited dataset availability. In addition, a time-consuming annotation phase on a subset of acquired images is generally required prior to the development of a model for a specific PA on which an SRF-OCC survey is to be carried out, as a data discrepancy usually appears between different OCC surveys. This is generally caused by both survey (camera angle, image resolution, flight altitude) and environmental factors (natural imbalance of species, landscape heterogeneity).

Pending the development of foundation DL models trained on massive amounts of aerial images, there is a strong need to develop efficient approaches for integrating existing DL models into the aerial survey process. This will reinforce the efficiency of the OCC method and reduce the associated cost by lightening the workload of human interpreters. The goal of this paper was to answer the following research question: Does a semi-automated approach requiring minimal human effort increase the accuracy and/or precision of population estimates compared to the traditional RSO approach? This paper presents the results of the first semi-automated aerial image processing pipeline applied on SRF-OCC images over a large and heterogeneous PA in Ivory Coast.

2. Materials and methods

2.1. Study area

The study area is the Comoé National Park located in Ivory Coast, which covers 11,488 km^2, making it the third biggest PA of west Africa. The CNP is covered at 64.3% of shrub savanna, 24.3% of wooded savanna and 7.6% of open forest. In addition, with patches of dense dry forest located in the south of the CNP as well as gallery forests along the shorelines of both Comoé and Iringou rivers, the CNP is an example of transitional habitats between forest and savanna. The park belongs to the 'northern plateaux' geophysical region (average altitude of 300 m) and is locally dominated by a number of reliefs, such as north-south-trending greenstone hills and bars rising to 500–600 m in the north-central and north-western regions; and tabular mounds with armored summits on shale, locally exceeding 500 m, in the south-east. The climate in this region is tropical savanna with dry winters (Aw). Due to its high diversity of habitats, the CNP is an important biodiversity reservoir (Hennenberg et al., 2006) and contains populations of wild terrestrial mammals, such as the roan antelope (*Hippotragus equinus* ssp. *koba*), the western hartebeest (*Alcelaphus buselaphus* ssp. *major*), or the buffalo (*Syncerus caffer* ssp. *brachyceros*), as well as endangered species such as the elephant (*Loxodonta africana*) (Fischer et al., 2002) and the emblematic chimpanzee (*Pan troglodytes* ssp. *verus*).

2.2. Aerial survey

Following previous aerial survey protocols of the CNP, the latter has been divided into four strata (Fig. 1): North-West (NW), North-East (NE), South-West (SW) and South-East (SE). Following standard SRF guidelines, 156 transects of 2 km spacing were oriented north-west to south-east in the northern strata, and north-east to south-west in the southern strata, covering 13% of the area. These orientations followed the ecological gradient of the area (rivers and mountains) while avoiding the aircraft pilot to be glared by the sun during the flights. Twelve days totaling 54 flight hours were needed to cover the entire CNP, starting on April 2 and ending on April 17, 2022.

The aircraft was a Cessna 206 (registration 5Y-AKP) and the flying crew was composed of: a pilot, an independent front-seat observer, two rear-seat observers (RSOs) and a photography manager. The same crew operated throughout the survey. During flights over the transects, RSOs were instructed to report the number of individuals and the associated species observed between the two strip markers placed on each of the aircraft's struts. The start and end of the transects were announced by the pilot. The front-seat observer was in charge of recording observations from the RSOs and their geo-locations on a tablet computer using the CyberTracker[1] app (v3.520). The photography manager managed the two oblique cameras set to acquire aerial imagery continuously and was also in charge of manually recording observations on papers for back-up. It is worth mentioning that due to a lack of space in the aircraft cabin, additional RSO cameras for large group bias correction (CITES-MIKE, 2020; PAEAS, 2014) have not been used during the survey.

From the multiple species counted during the survey, only seven species usually surveyed by aircraft, in fairly large numbers and/or of conservation interest were selected for this study. These species are referred to as 'key species' in the text and include western hartebeest, buffalo, kob (*Kobus kob* ssp. *kob*), waterbuck (*Kobus ellipsiprymnus* ssp. *defassa*), elephant, roan antelope and warthog (*Phacochoerus africanus* ssp. *africanus*).

Transect (or sample unit) area were estimated using the height above ground level and a theoretical predefined strip-width of 150 m on each side of the aircraft at a flight altitude of 91.4 m (300 ft) (CITES-MIKE, 2020; Craig, 2012; Norton-Griffiths, 1978; PAEAS, 2014). The height above the ground level as well as associated geo-location were recorded each second during the flights by a LightWare SF30/D laser altimeter. The strip width was calibrated using 20 ground-marks placed 20 m apart on either side of the runway. Thirty crossings of the aircraft at increasing height above ground level (between 55 and 208 m) were carried out, during which the number of marks appearing between the strip markers was counted.

2.3. Cameras and image acquisition

Two Nikon D5600 24-megapixel digital reflex cameras equipped with Nikkor AF-S 18–55 zoom lenses were positioned inside the aircraft, one on each side, using articulated double suction cups fixed on the windows. The cameras were mounted obliquely at an inclination of 36.5° and zoom lens were set and taped at 35 mm to capture a strip of about 150 m width, in accordance with SRF standards (CITES-MIKE, 2020; Craig, 2012; PAEAS, 2014) and recent OCC studies (Lamprey et al., 2020a, 2020b). The camera angle was chosen to be as close as possible to the angle of vision of human observers while intercepting the strip markers at the inner and outer edges of the images. External intervalometers were used and set to acquire images at 2 s intervals, to ensure overlapping coverage at a ground speed of 160 km/h. Based on initial field trials, cameras were set to 'aperture-priority' mode, with aperture set to f/5.0, the auto-ISO was preferred, with a minimum value of 500, and minimum shutter speed was set to 1/2000 s. In total, 190,686 images were saved in 6000 × 4000 pixels JPEG format, from which 148,239 appeared on transect after cleaning. All images were geo-referenced in UTM coordinates using the GeoSetter[2] software which associated the altimeter's GPS tracklog to the exact acquisition time of each image.

2.4. Deep learning model

The DL architecture HerdNet[3] (Delplanque et al., 2023a) has been selected for processing the aerial survey images given its attractive performances on a previous SRF-OCC study (Delplanque et al., 2023b). HerdNet is a single-stage fully convolutional neural network built with two heads: one dedicated to the accurate point detection of animals in the image and the other to their classification.

HerdNet was trained multiple times during image processing, for progressively fine-tuning it to the study area landscape and species. For each training stage, we constructed an unbiased validation set comprising 20% of the current dataset's images. Each set was carefully designed to maintain a similar distribution of species and to ensure independence by keeping images from the same transect grouped together. This avoided as far as possible any performance bias related to the natural imbalance of species, and any spatial bias related to the overlap of images. As for the hyperparameters, we set training patch size to 512 × 512 pixels, the minibatch size to 8 patches, the learning rate to 10^{-6}, the weight decay to 5×10^{-4} and the number of epochs to 200 or 50, depending on the training schedule (see section 2.5.2 below). Horizontal flipping and motion blur have been used as data augmentation, with a 50% probability of occurrence. To avoid any risk of overfitting at each training stage, we selected the model relative to the epoch that gave the best performance on the validation set. During inference, the patch size was set to 1024 × 1,024 pixels to accelerate the process. Further information on the fine-tuning process is described in section 2.5.2.

2.5. Image processing

Images have been processed through the use of the DL model coupled with human manual interpretation steps. This 'human-assisted' DL-based image processing pipeline has been designed to minimize human effort while maximizing the quality of counting results. In the following sections, this approach is referred to as the Semi-Automated Deep Learning (SADL) model, and SADL-OCC refers to the integration of the SADL model with the OCC technique. This section therefore presents the main components and steps of this developed approach.

2.5.1. Semi-automatic loop

The core component of the pipeline was the Semi-Automatic Loop (SAL), which integrates both the DL model and a human-expert interpreter. The SAL operated by taking aerial images as input and passing them through the DL model to harvest point detections. Subsequently, it conducted a 256 × 256 pixel crop, centered on each detection, generating thumbnails that received a rapid examination during the initial human verification step. This verification step entails manually classifying each thumbnail as either False Positive (FP), True Positive (TP), or uncertain object (Fig. 2).

This first human verification step played a crucial role in significantly reducing the number of full-size images requiring review, thereby minimizing the overall analysis time. Additionally, this step served as a guide for the interpreter, directing attention to the most relevant detections (i.e. TP). After this step, the relevant detections were projected back into their original full-size images for a second verification. In the second human verification step, the interpreter thoroughly examined

[1] https://cybertracker.org/

[2] https://geosetter.de/

[3] https://github.com/Alexandre-Delplanque/HerdNet

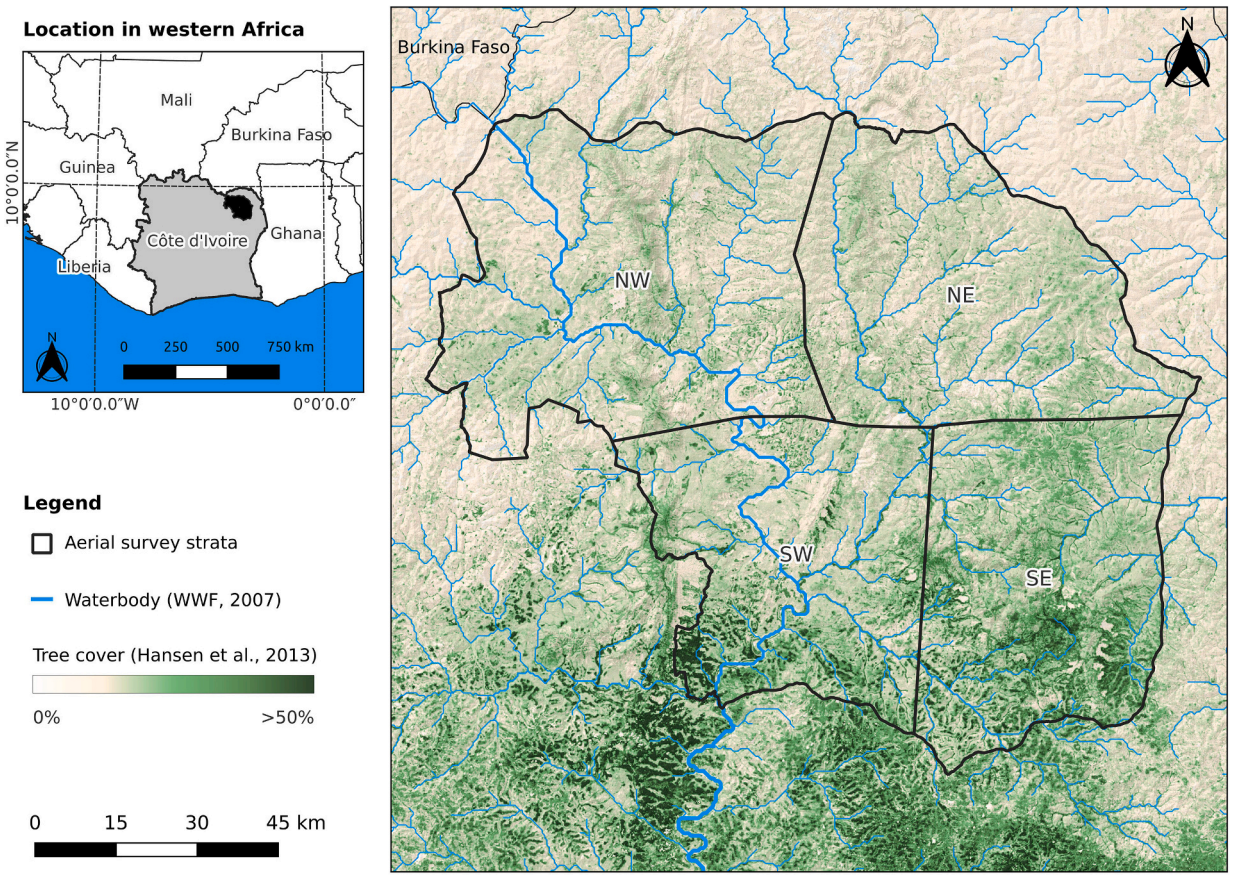

Fig. 1. Map of the Comoé National Park and survey area strata: North-West (NW), North-East (NE), South-West (SW) and South-East (SE). Waterbody was derived from the river network map for Africa produced by the World Wildlife Fund (2007) and the tree cover from the map of Hansen et al. (2013).

the entire image to point out any potentially missed animals and, if necessary, had the option to rectify the predicted identification (species name) and/or point coordinates (Fig. 2). The second step has been done on Label Studio 1.3 (Tkachenko et al., 2020) through a custom template.

2.5.2. *Model fine-tuning and inference*

In aerial surveys of PA using the OCC technique, the availability of a region-specific DL model, encompassing the PA's unique species and landscape characteristics, remains limited as these approaches are still emerging and such data are often sensitive. Consequently, a pre-trained DL model is needed. Such a model has been trained on images from a different source (e.g. another PA) but following a similar task (e.g. detecting terrestrial mammals in oblique aerial imagery). Ideally, the pre-trained model should originate from a similar PA containing similar target species and following the same acquisition standards to achieve optimal results. Nevertheless, it is essential to recognize that while these pre-trained models may yield reasonably accurate predictions at times, they are not entirely reliable and risk losing accuracy as the discrepancy between source and target data widens. Therefore, a crucial step involves fine-tuning the model to suit the targeted PA. As some researchers shared their model in recent years (Delplanque et al., 2022, Delplanque et al., 2023a; Eikelboom et al., 2019), we propose a simple yet effective method that could be applied across various cases.

It is essential to select the most densely populated region to guarantee a sufficient number of instances per species for the optimal fine-tuning of the DL model. In this study, the SW stratum was selected, which encompassed three distinct flights conducted over three consecutive days.

Regarding the pre-trained model, we utilized the DL model developed by Delplanque et al. (2023a) that was initially fine-tuned on images acquired in a survey of Queen Elizabeth National Park, Uganda (Lamprey et al., 2023) following OCC procedures developed in Murchison Falls National Park, Uganda (Lamprey et al., 2020a). The data acquisition conditions closely resembled the current study's data acquisition process, encompassing similar wildlife species.

The pre-trained model underwent inference and fine-tuning for 4 iterations using the entire SW stratum employing the SAL. This iterative process served to enhance the model's performance and gather samples pertaining to each key species present in the region. The training procedure for the two first fine-tuning iterations was the one proposed in the original paper (Delplanque et al., 2023a) which consisted of two main steps: 1) training the architecture using positive patches for 200 epochs, and 2) collecting and including hard negative patches, which are patches containing false positives, to further train the model for 50 epochs in order to reduce the number of false positives. During the two last fine-tuning iterations, only the second step of the training procedure was used. Hard negative patches were created using false positives that emerged from the thumbnail classification (step 1 of the SAL). To avoid a too severe imbalance between positive and negative patches the batch was equally balanced between the latter during training.

Once the fine-tuning process was done, the model was inferred on images from the other strata. The detections resulting from this inference were subjected to verification using the SAL. To both maximize the probability of detecting all species individuals and take advantage of the collected verified detections, the model was trained one last time on the entire set of verified images and then inferred on all 148,239 transect images for a final verification. From this process, the previously unseen images were verified using the SAL.

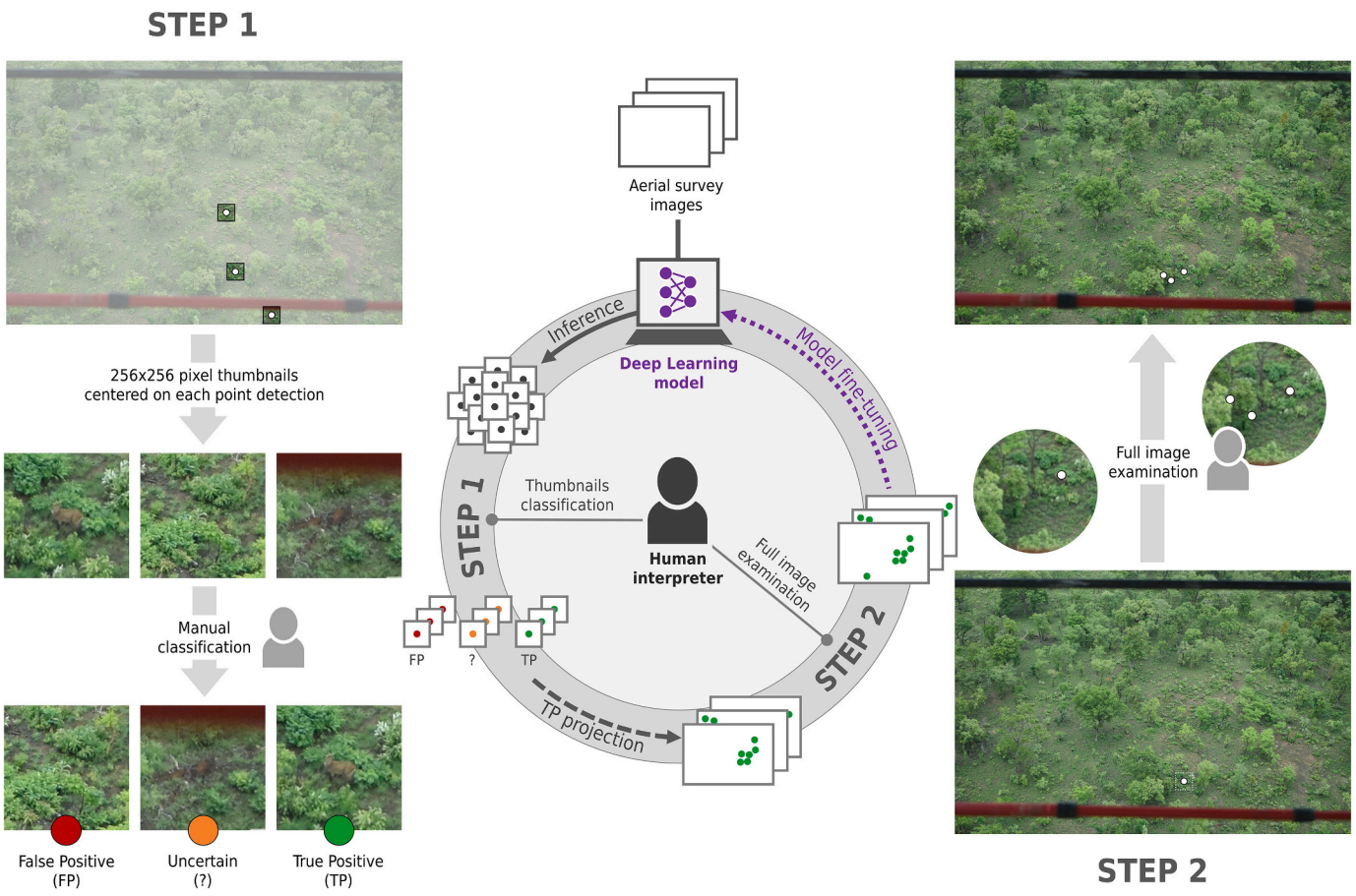

Fig. 2. Overview of the semi-automatic loop (SAL). The central part of the figure is a schematic representation of the loop, and the sides illustrate the two main steps on a sample image of the aerial survey. TP and FP referred to True Positive and False Positive respectively.

2.5.3. *Duplicate removal*

Due to overlapping coverage of images, the same animal may be present in multiple images, which may lead to an overestimation of the true number of individuals. It was therefore necessary to carefully manage consecutive images to avoid double counting. This has been done on Label Studio 1.3 (Tkachenko et al., 2020) by a human operator who manually reviewed consecutive images and assigned an additional label to the detections to distinguish and discard duplicates.

2.6. *Data analysis and population estimate*

Prior to comparing RSO and SADL-OCC approaches, counting bias was checked between right and left RSOs. For each species and stratum, the number of groups encountered as well as the number of animals counted in the groups were compared using a chi-square test and a Mann-Whitney *U* test, respectively (CITES-MIKE, 2020).

RSO and SADL-OCC counting results were analyzed using the Jolly II method for unequal sized sample units (Jolly, 1969), where the transects were the sample units, following the guidelines of Norton-Griffiths (1978). As the survey area was stratified, the method of Jolly II was applied on each stratum. The population estimates and variances were calculated for each stratum, and these were then added together to obtain estimates for the whole survey area. The global standard error was calculated by taking the square root of the summed variances (Norton-Griffiths, 1978). To compare the RSO and SADL-OCC surveys, the null hypothesis that estimates were not significantly different ($\alpha = 0.05$) was tested by calculating *d* as:

$$d = \frac{\widehat{Y}_S - \widehat{Y}_R}{\sqrt{\sigma_S^2 + \sigma_R^2}} \quad (1)$$

Where $\widehat{Y}_S$ and $\widehat{Y}_R$ are the population estimates of SADL-OCC approach and RSOs respectively, and σ_S^2 and σ_R^2 are their variance (Norton-Griffiths, 1978). Where $d > 1.96$, the result is statistically significant at alpha = 0.05.

RSO and SADL-OCC approaches were also compared using the paired *t*-test and the non-parametric Wilcoxon signed-ranks test, where the samples were the transects (Lamprey et al., 2020b).

Finally, in order to evaluate and explain potential counting differences between SADL-OCC and RSO, 50 RSO observations were randomly selected for each of the following group size class announced by RSOs: 1) 1 to 5 animals, 2) 6 to 10 animals, 3) 11 to 20 animals and 4) 21 and more animals. At each of these 200 locations, an experienced human operator compared the RSO count with the SADL-OCC count. An explanation of the differences observed was provided following a visual analysis of the matching images (Fig. 3) as follows: 1) part of the group is probably hidden by vegetation, 2) a suspected counting error of RSOs, 3) part of the group is out-of-strip on the matching images, 4) the group was missed by the SADL-OCC approach or 5) the group observed by RSO does not appear on the matching images.

3. Results

3.1. *RSOs consistency and Jolly II analysis*

Testing consistency between right and left RSO indicated no significant differences in encounter rates for the western hartebeest, kob,

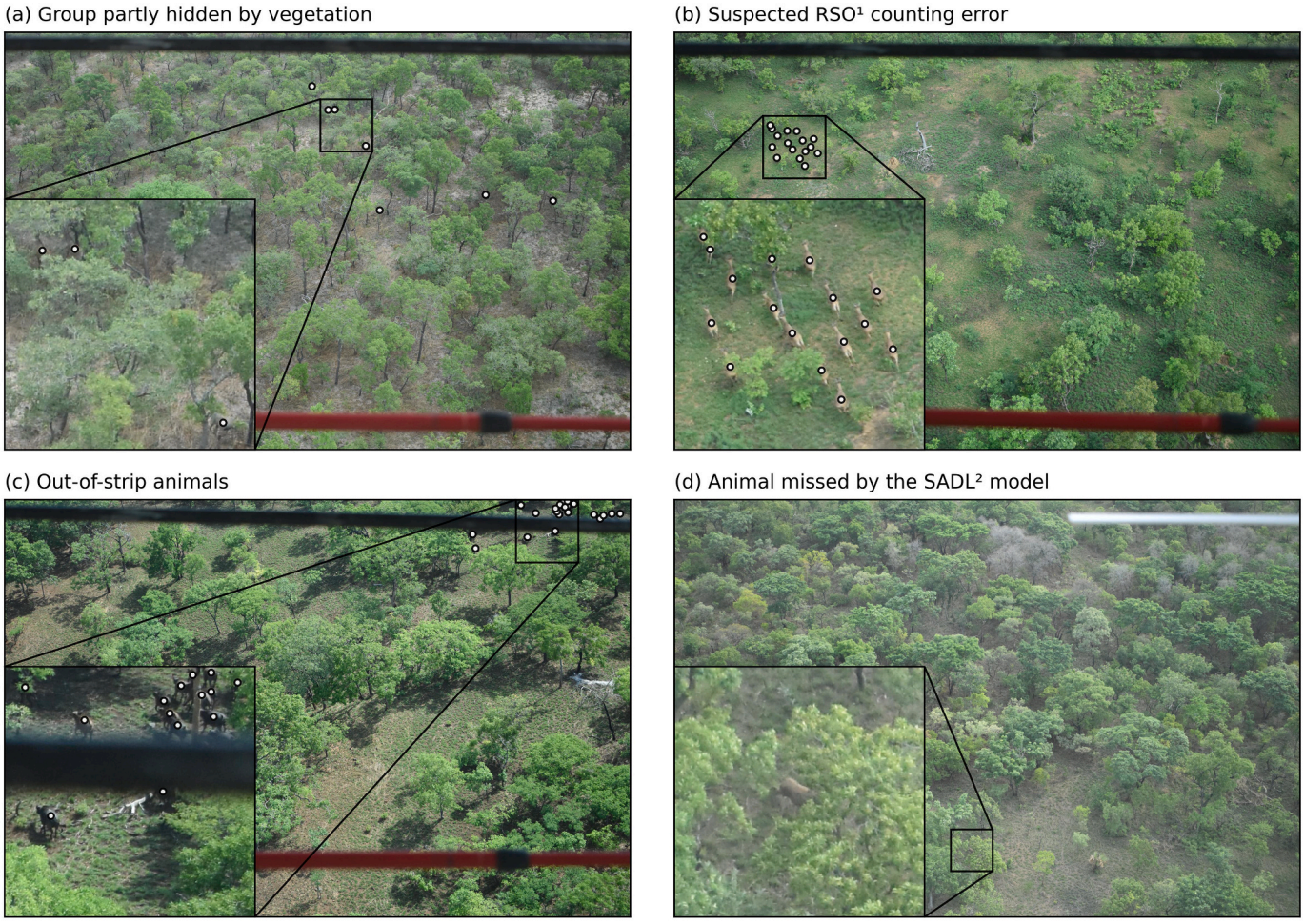

Fig. 3. Illustration of differences observed between the SADL-OCC and RSO approaches for 200 random RSO observations: (a) a group of 7 roan antelopes detected by the SADL-OCC approach, where some individuals were probably hidden by trees since the RSO announced a group of 35 individuals, (b) a group of 17 western hartebeests estimated at 20 individuals by the RSO indicating a probable RSO counting error, (c) a group of buffalo where most of the individuals appeared out-of-strip in the SADL-OCC approach, but where all individuals were counted in-the-strip by the RSO, and (d) an example of image containing a roan antelope missed by the SADL-OCC approach.

waterbuck, elephant and warthog. The exceptions were for roan antelope in SW stratum with 21 (right) and 7 (left) encounters ($\chi 2$=7.00, d.f. = 1, $P = 0.008$) and buffalo in SE stratum with 5 (right) and 0 (left) encounters ($\chi 2$=5.00, d.f. = 1, $P = 0.025$). Concerning the number of animals reported, only buffalo in SE stratum and waterbuck in SW stratum showed a significant difference. Median buffalo counts of right and left RSO were 35 and 0, respectively ($U = 0$, n1 = 5, n2 = 0, $P < 0.001$) while median waterbuck counts were 1 and 3 ($U = 1$, n1 = 5, n2 = 3, P = 0.025).

The Jolly II analysis showed that SADL-OCC population estimates were significantly higher than RSO ones for small-sized species, i.e. kob and warthog, and not significantly different for the other key species (i.e. elephant, buffalo, western hartebeest, roan antelope and waterbuck). Similarly, results of the paired transect *t*-test and the non-parametric Wilcoxon signed-ranks test indicated the same trend (Table 1). For kob and warthog, the difference in estimates was highly significant ($p < 0.001$) with tighter confidence intervals, indicating that the SADL-OCC approach counted much more individuals than RSOs and that the counts were more consistent across the survey area. SADL-OCC estimates for kob, warthog and buffalo were respectively 240%, 163% and 17% higher than RSO estimates, while being lower for roan antelope (−19%), western hartebeest (−7%), and waterbuck (−2%). While the elephant population was unfortunately too small for drawing valid consideration, the results showed that the SADL-OCC approach found and correctly counted the two groups observed during the aerial survey.

The SADL-OCC approach estimates are systematically higher than RSOs for each key species in western strata (i.e. NW and SW), while the inverse trend was observed for eastern strata (i.e. NE and SE), except for buffalo, kob and warthog where the results vary. For instance, SADL-OCC buffalo estimates are nearly two times higher than RSO ones in the NW stratum, but nearly three times lower in the SE stratum (Table 1).

3.2. Counting differences

Based on the additional analysis of 200 randomly-selected RSO observations, 35 instances (17.5%) of mutual agreement with the SADL-OCC approach were observed, ranging from 1 observed animal to a group of 16 individuals. This leaves 165 instances (82.5%) where differences were observed. These differences were mainly explained (35.8%) by the presence of relatively dense vegetation (Fig. 4), hiding some individuals of the group in the image. The second most observed situation (26.7%), was a group of animals observed by RSOs but not found on images, which often contained highly vegetated scenes. The third explanation (24.2%) of differences was the suspected error of RSOs when estimating the group of animals they observed. Finally, animals of

Table 1
Jolly II estimates ($\hat{Y}$) and standard error (SE) for SADL-OCC[1] ($\hat{Y}_S$) and RSO[2] ($\hat{Y}_R$) surveys of key species in Comoé National Park, using the stratified statistical scheme, and results of the d-statistic (Norton-Griffiths, 1978) and the paired transect *t*-test (df = 154) and Wilcoxon signed-ranks test for comparison. The final column indicates the extent to which SADL-OCC estimates are superior to RSO estimates, and was calculated as $\Delta\% = (\hat{Y}_S/\hat{Y}_R) - 1$ (Lamprey et al., 2020b).

	North-West		North-East		South-West		South-East		Total			SADL-OCC vs RSO					
Species	$\hat{Y}_S$ (SE)	$\hat{Y}_R$ (SE)	$\hat{Y}_S$ (SE)	$\hat{Y}_R$ (SE)	$\hat{Y}_S$ (SE)	$\hat{Y}_R$ (SE)	$\hat{Y}_S$ (SE)	$\hat{Y}_R$ (SE)	$\hat{Y}_S$ (SE)	$CI_{95\%}$	$\hat{Y}_R$ (SE)	$CI_{95\%}$	d-stat	p	t-stat	p	W	p	Δ%
Western hartebeest	5243 (713)	4972 (869)	2287 (274)	2630 (428)	7716 (546)	7424 (901)	2316 (356)	3793 (621)	17,562 (1005)	± 11%	18,819 (1461)	± 15%	−0.709	0.479	0.979	0.329	2918	0.386	−7%
Buffalo	425 (200)	220 (105)	9 (6)	9 (6)	2669 (754)	1852 (710)	284 (190)	813 (476)	3387 (803)	± 46%	2894 (861)	± 58%	0.419	0.676	−0.308	0.759	140	0.775	17%
Kob	1743 (381)	520 (187)	454 (126)	213 (107)	7766 (799)	2102 (425)	181 (54)	142 (70)	10,143 (896)	± 17%	2977 (482)	± 32%	7.045	<0.001	−4.592	<0.001	432.5	<0.001	241%
Waterbuck	249 (77)	73 (44)	250 (76)	694 (261)	893 (160)	275 (123)	168 (66)	542 (176)	1559 (204)	± 26%	1585 (341)	± 42%	−0.064	0.949	0.123	0.902	535.5	0.159	−2%
Elephant	0 (0)	0 (0)	0 (0)	0 (0)	275 (133)	225 (109)	0 (0)	0 (0)	275 (133)	± 95%	225 (109)	± 95%	0.290	0.772	−1.419	0.158	0	0.157	22%
Roan antelope	930 (255)	820 (239)	500 (88)	833 (236)	1560 (210)	1535 (300)	755 (210)	1432 (404)	3745 (401)	± 21%	4621 (605)	± 26%	−1.206	0.230	1.408	0.161	1011	0.687	−19%
Warthog	849 (158)	278 (99)	111 (29)	46 (30)	1785 (209)	584 (125)	200 (71)	213 (97)	2946 (273)	± 18%	1121 (189)	± 33%	5.498	<0.001	−4.078	<0.001	328	<0.001	163%

[1] SADL-OCC, semi-automated deep learning oblique-camera-count;
[2] RSO, rear-seat observer.

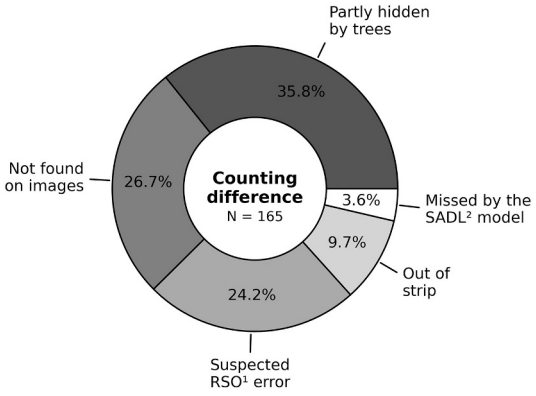

¹RSO, rear-seat observer; ²SADL, semi-automated deep learning.

Fig. 4. Distribution of explanatory causes for differences in counts observed between the SADL-OCC and RSO approaches. The percentages were calculated from the 165 random observations showing differences in counts. Mutual agreements (i.e. no differences) were observed for 35 observations.

the group that appeared out-of-strip on the image(s) explained around 9.7% of the differences, and animal or group of animals missed by the SADL-OCC approach (total of 22 animals) explained 3.6%. It should be noted that the presence of vegetation is an explanatory cause that cannot be excluded for the others, and may be a secondary explanation of the difference observed.

Comparing the sample of 200 RSO count values with those derived from the SADL-OCC approach for each key species, it was observed that in most cases large groups were underestimated by the SADL-OCC approach (Fig. 5). This was mainly due to the vegetation cover, the absence of the group in the acquired images and because part of the groups appeared out-of-strip in the images. The resulting differences were particularly severe for the groups observed in the SE and NE strata and for large groups (> 20 animals) of western hartebeest, buffalo, waterbuck and roan antelope (Fig. 5).

3.3. Human effort

The human time investment in the SADL-OCC approach was around 111 h. More than half of this time was devoted to full examination of the 24 megapixel (MP) images (i.e. step 2 of the SAL), a third to classifying the thumbnails (i.e. step 1 of SAL) and around 10% to removing duplicates in overlapping image areas (Table 2). Considering a 8-h working day, the total time is equivalent to 14 working days for one person. Nevertheless, most of the work was done by one machine through the DL model, which devoted around 530 h to all the required processing, i.e. inference and fine-tuning.

Assuming a manual interpretation time of a few minutes per 24MP image (Lamprey et al., 2020a), it would take thousands of hours for one person to process the 148,239 transect images. The use of the SADL model thus represents a significant time saving compared to a fully manual interpretation. Furthermore, when comparing the total cumulative counting time of the 3 observers (162 h) with the human time invested in the SADL-OCC approach (54 h for the photography manager and 111 h for DL model's detections verification), the SADL-OCC approach required similar human effort than the traditional SRF approach.

4. Discussion

As DL models are not yet ready for fully automatic use on aerial survey images, we propose a semi-automatic DL approach that tackles the main limitation of the OCC technique: the considerable time required by humans to interpret images. To the best of our knowledge,

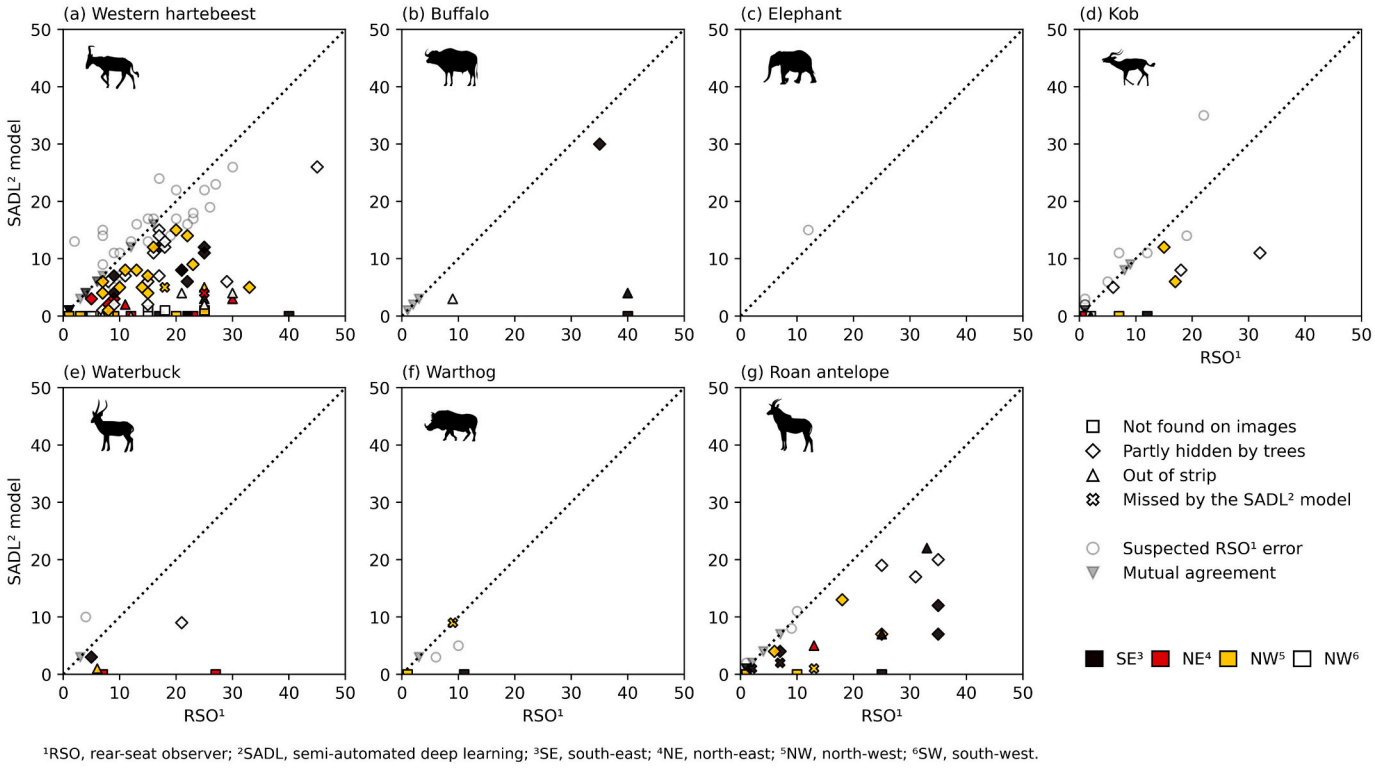

Fig. 5. Scatter plots between count values announced by RSOs and those derived from the SADL-OCC approach, for each key species. These plots were constructed on the basis of the 200 random RSO observations examined visually. Point markers are differentiated according to the most likely explanatory cause and shaded according to the strata.

Table 2
Detail of the human workload involved in the SADL-OCC detection verification process.

	Number of items		Allocated time	
Human task	**First pass**	**Final pass**	**Total (relative share)**	**8 h-workday equivalent**
Thumbnails classification	85,779 thumbnails	93,472 thumbnails	24.0 h (33%)	4.7 days
Full 24MP image examination	3188 images	529 images	64.3 h (58%)	8.0 days
Duplicate removal	1739 images	163 images	9.5 h (10%)	1.1 days

this is the first time that DL has been integrated into an aerial camera survey at such a large-scale study area in Africa to produce population estimates. Our results showed that the SADL model significantly reduced the human interpretation workload while providing as good or even better population estimates than those obtained from RSOs counts. The SADL-OCC approach seems to be well adapted to count small-sized static species, as revealed by the high estimates for kob and warthog. However, it is difficult to draw conclusions about the larger and more mobile species.

4.1. Population estimates

Unlike previous African OCC studies (Lamprey et al., 2020a, 2020b), we did not observe a systematic significant positive difference between RSO population estimates and those derived from imagery counts for each key species. While the DL model performance could be the first likely explanation, our thorough comparison of 200 RSO and SADL matching counts highlighted that the vegetation was the main cause of the observed differences and that model errors were the least one. The CNP is indeed a vegetated PA and thus differs from arid and semi-arid areas where animals are much more easily captured by oblique cameras, even when running, as they are less prone to tree occlusion. We hypothesize that SADL-OCC approach performance should increase in open areas. Nonetheless, as no additional cameras were used to correct RSO counts for large groups, we may not reject the possibility of biased estimation from RSOs.

The SADL-OCC approach gave lower estimates compared to RSOs in eastern strata, particularly for western hartebeest, buffalo, waterbuck and roan antelope. These differences are mainly explained by the vegetation which occluded the few groups observed by RSOs during the survey. Given the lower animal density in these regions, the observed difference had a significant impact on the overall population estimates.

It should also be added that western hartebeest, buffalo and roan antelope often showed a running reaction to the passing aircraft, making them more detectable to RSOs due to movement. Whereas an RSO can easily estimate a group of moving animals because he has a continuous view of the scene, the OCC method has a fixed sampled view. This would explain why kob and warthog were better estimated by the SADL-OCC approach, as these species have a much more static behavior. This staticity also complicates the task of RSOs, and increases the risk of missing individuals during flights.

4.2. Method comparison

Our semi-automatic approach went far in addressing the main limitation of the OCC method, i.e. the time-consuming burden of image interpretation (Bröker et al., 2019; Lamprey et al., 2020b), whilst providing at least similar population estimates than the traditional RSO approach. In addition, this combination of DL model and OCC method seems to better detect small-sized and static animals, reducing the variance in counts between transects and therefore tightening the confidence interval of the estimate. Thanks to the cameras and the SAL,

what has been counted and identified during the aerial survey was recorded, increasing the validity of the estimates obtained and enabling further checking and potential certification.

The role of human interpreter in the semi-automatic approach is crucial, as he thoroughly verifies the DL model predictions and therefore gives confidence in the final count values. While the use of a DL model reduces traditional aerial survey bias such as animal size and color, group size or density, and observer fatigue (Griffin et al., 2013; Jachmann, 2002; Norton-Griffiths, 1976; Wal et al., 2011), the work of the human interpreter helps to reduce DL model counting bias appearing in heterogeneous scenes where many false alarms may be generated (Delplanque et al., 2023b).

>70% of the counting difference between RSOs and the SADL-OCC approach were explained by environmental and acquisition factors, and <4% by the DL model performance. These results highlight some shortcomings of our OCC protocol. First, as stated in section 4.1, the fixed and sampled time window of the OCC method makes it impossible to count animals running under sparse canopy, unlike RSOs, which seemed to easily adapt to animal movements through continuous observation. A shorter time interval between image footage might enable better capture of animal movement, and therefore better estimation. Secondly, even though the RSOs have been instructed to count the animals in the strip perpendicular to the line of flight, the front-seat observer's announcement of a group instinctively guided them to look slightly forward to give a better estimate. This, combined with vegetation cover and animal's perturbation due to the overflight aircraft, could explain why we didn't find part or entire groups on concurrent images with the OCC method. While these assumptions were impossible to validate in our study, they could be verified in future research by using additional RSO cameras (CITES-MIKE, 2020; PAEAS, 2014). This will allow refine the counts and reject RSO observations absent from the images. Finally, turbulence during flight at 92 m (300 ft) height had obviously an impact on image footage and may explain the proportion of animals counted 'out-of-strip' by the SADL-OCC approach. Nevertheless, we observed that when a strip marker crossed a large group of animals, RSOs had difficulty estimating the number of animals in and out the strip, often leading to an overestimation of animals counted in the strip. This effect might be exacerbated by turbulence, causing the aircraft to rock and the strip to vary.

Concerning the effect of vegetation, future work should further study the relationship between vegetation cover and animal counting in aerial images. In addition, video recording and analysis might be considered in highly vegetated areas to better capture the movement of groups under spare canopies.

4.3. New insights for aerial surveys

Our study opens up promising perspectives for frequent monitoring and mitigation effort in PAs since OCC survey results may now be obtained rapidly with the use of our semi-automatic approach. Given that the SADL-OCC approach gave similar or even better estimates for small-sized species compared to RSOs, and following previous OCC results (Delplanque et al., 2023b; Lamprey et al., 2020a, 2020b; Lamprey et al., 2023), we suggest that aerial survey standards are moved forward to embrace new technologies.

We believe that the observer work could be migrated from on-sight count to DL model detection verification, which could considerably reduce associated costs given that during an aerial survey, RSOs are generally mobilized full time for several weeks. Verifying DL model predictions (i.e. points) is an easier task than on-sight counting and does not require highly experienced interpreters who can be easily and rapidly trained. Furthermore, unlike on-sight counting, detection verification may be spread over several people and spaced out over time to avoid any effect of human fatigue on counting results. However, for an autonomous use by PAs, the proposed approach requires a workstation with a good Graphic Processing Unit (GPU) (i.e. at least 8GB of memory), and a dedicated and experienced person in charge of model fine-tuning and inference.

Pending the development of long-endurance Unpiloted Aerial Vehicles (UAVs), our proposed method has a great potential for the use of microlight aircrafts in aerial surveys. Compared to 4-(6-)seat Cessna light aircraft, microlight aircrafts are a much affordable option for PA managers since they are cheaper, they require less expensive fuel and maintenance, and they have less stringent pilot licensing regulations. The main obstacles to their use in wildlife aerial surveys have been their limited capacity of 1 or 2 people and their poor stability at low altitude, making it impossible to apply the traditional method with RSOs. However, our results and those of previous image-based studies (Lamprey et al., 2020b; Lethbridge et al., 2019) showed that observers may be replaced by oblique cameras, since image interpretation burden should now mainly be handled by semi-automated DL models. Thanks to high-resolution cameras (e.g. 36MP), it is then possible to fly higher, which will 1) ensure flight stability and therefore human safety, 2) increase the sampling rate at no extra flying time and costs, thus providing more accurate estimates (Norton-Griffiths, 1978) and 3) mitigate the effect of running animals thanks to a large image footprint and thus a greater scope for movement. Coupling these cameras with Inertial Measurement Units (IMU) and Global Navigation Satellite Systems (GNSS) would enable image ground projection from which more precise transect area estimates could be derived (Lisein et al., 2013), thus eliminating the need for strip markers.

5. Conclusions

Will AI revolutionize wildlife aerial survey? Our results suggest that we are heading in this direction. Most of our observations regarding the differences observed between RSO and SADL-OCC approaches point to the need to refine the OCC protocol more than improving the semi-automatic approach. While the proposed methodology needs to be validated in other PAs and our OCC protocol further refined, the significant time saving compared to a fully manual image interpretation is a major step towards revolutionizing aerial surveys in Africa.

Funding information

The work of Alexandre Delplanque was supported under a grant from the Fund for Research Training in Industry and Agriculture (FRIA, F.R.S.-FNRS). This study has been possible with the financial support of the German Financial Cooperation through KfW (BMZ n°2014 68 222/ n°2019 67 199) to the Comoé National Park Biodiversity Protection Project, Phase II. This project was promoted by the OIPR through its North-East Zone Directorate (DZNE), with technical assistance from AHT GROUP GmbH, leader of the consortium with AMBERO Consulting GmbH and the Swiss Center for Scientific Research.

CRediT authorship contribution statement

Alexandre Delplanque: Writing – review & editing, Writing – original draft, Visualization, Software, Methodology, Investigation, Formal analysis, Data curation, Conceptualization. **Julie Linchant:** Writing – review & editing, Investigation, Data curation, Conceptualization. **Xavier Vincke:** Writing – review & editing, Investigation, Conceptualization. **Richard Lamprey:** Writing – review & editing, Investigation, Conceptualization. **Jérôme Théau:** Writing – review & editing. **Cédric Vermeulen:** Writing – review & editing. **Samuel Foucher:** Writing – review & editing. **Amara Ouattara:** Writing – review & editing. **Roger Kouadio:** Writing – review & editing. **Philippe Lejeune:** Writing – review & editing, Supervision, Resources.

Declaration of competing interest

The authors declare that they have no known competing financial

interests or personal relationships that could have appeared to influence the work reported in this paper.

Data availability

The data that has been used is confidential.

Acknowledgements

The authors would like to thank Colonel-Major Adama Tondossama, director general of OIPR, the pilot Alexis Peltier and the observers Nounifou Sabdano, Théophile Ayeby and Yves Constant Koffi Kouassi. The authors gratefully acknowledge the Uganda Conservation Foundation, Richard Lamprey and Alexandre Delplanque for the use of their wildlife detection model developed in 2022 during the preliminary detection stage of this work. This model was initially trained on oblique aerial images of the Queen Elizabeth Protected Area (Uganda), acquired in September 2018 whose aerial survey was funded by Uganda Conservation Foundation, Global Conservation, Save the Elephants, Vulcan Inc. and the Uganda Wildlife Authority. Species silhouettes used in the manuscript were sourced from https://www.phylopic.org/. The western hartebeest and waterbuck silhouettes are from Jan A. Venter, Herbert H. T. Prins, David A. Balfour & Rob Slotow (vectorized by T. Michael Keesey), available under the CC-BY 3.0 license (https://creativecommons.org/licenses/by/3.0/), all other silhouettes have been dedicated to the public domain.

References

Bröker, K.C.A., Hansen, R.G., Leonard, K.E., Koski, W.R., Heide-Jørgensen, M.P., 2019. A comparison of image and observer based aerial surveys of narwhal. Mar. Mamm. Sci. 35 (4), 1253–1279. https://doi.org/10.1111/mms.12586.

Cardinale, B.J., Duffy, J.E., Gonzalez, A., Hooper, D.U., Perrings, C., Venail, P., Narwani, A., Mace, G.M., Tilman, D., Wardle, D.A., Kinzig, A.P., Daily, G.C., Loreau, M., Grace, J.B., Larigauderie, A., Srivastava, D.S., Naeem, S., 2012. Biodiversity loss and its impact on humanity. Nature 486 (7401). https://doi.org/10.1038/nature11148. Article 7401.

Caughley, G., 1974. Bias in aerial survey. J. Wildl. Manag. 38 (4), 921–933. https://doi.org/10.2307/3800067.

Ceballos, G., Ehrlich, P.R., 2023. Mutilation of the tree of life via mass extinction of animal genera. Proc. Natl. Acad. Sci. 120 (39), e2306987120 https://doi.org/10.1073/pnas.2306987120.

CITES-MIKE, 2020. Monitoring the Illegal Killing of Elephants: Aerial Survey Standards for the MIKE Programme. Version 3.0. Convention on International Trade in Endangered Species - Monitoring the Illegal Killing of Elephants Programme (CITES-MIKE), Nairobi, Kenya.

Craig, G.C., 2012. Aerial Survey standards for the MIKE Programme. Version 2.0. CITES MIKE programme.

Delplanque, A., Foucher, S., Lejeune, P., Linchant, J., Théau, J., 2022. Multispecies detection and identification of African mammals in aerial imagery using convolutional neural networks. Remote Sens. Ecol. Conserv. 8 (2), 166–179. https://doi.org/10.1002/rse2.234.

Delplanque, A., Foucher, S., Théau, J., Bussière, E., Vermeulen, C., Lejeune, P., 2023a. From crowd to herd counting: how to precisely detect and count African mammals using aerial imagery and deep learning? ISPRS J. Photogramm. Remote Sens. 197, 167–180. https://doi.org/10.1016/j.isprsjprs.2023.01.025.

Delplanque, A., Lamprey, R., Foucher, S., Théau, J., Lejeune, P., 2023b. Surveying wildlife and livestock in Uganda with aerial cameras: deep learning reduces the workload of human interpretation by over 70%. Front. Ecol. Evol. 11 https://doi.org/10.3389/fevo.2023.1270857.

Eikelboom, J.A.J., Wind, J., van de Ven, E., Kenana, L.M., Schroder, B., de Knegt, H.J., van Langevelde, F., Prins, H.H.T., 2019. Improving the precision and accuracy of animal population estimates with aerial image object detection. Methods Ecol. Evol. 10 (11), 1875–1887. https://doi.org/10.1111/2041-210X.13277.

Fischer, F., Gross, M., Linsenmair, K.E., 2002. Updated list of the larger mammals of the Comoé National Park. Ivory Coast. 66 (1), 83–92. https://doi.org/10.1515/mamm.2002.66.1.83.

Griffin, P.C., Lubow, B.C., Jenkins, K.J., Vales, D.J., Moeller, B.J., Reid, M., Happe, P.J., Mccorquodale, S.M., Tirhi, M.J., Schaberl, J.P., Beirne, K., 2013. A hybrid double-observer sightability model for aerial surveys. J. Wildl. Manag. 77 (8), 1532–1544. https://doi.org/10.1002/jwmg.612.

Grimsdell, J.J.R., Westley, S., 1981. Low-Level Aerial Survey Techniques. International Livestock Centre for Africa. https://cgspace.cgiar.org/handle/10568/4207.

Hansen, M.C., Potapov, P.V., Moore, R., Hancher, M., Turubanova, S.A., Tyukavina, A., Thau, D., Stehman, S.V., Goetz, S.J., Loveland, T.R., Kommareddy, A., Egorov, A., Chini, L., Justice, C.O., Townshend, J.R.G., 2013. High-resolution global maps of 21st-century forest cover change. Science 342 (6160), 850–853. https://doi.org/10.1126/science.1244693.

Hennenberg, K.J., Fischer, F., Kouadio, K., Goetze, D., Orthmann, B., Linsenmair, K.E., Jeltsch, F., Porembski, S., 2006. Phytomass and fire occurrence along forest–savanna transects in the Comoé National Park, Ivory Coast. J. Trop. Ecol. 22 (3), 303–311. https://doi.org/10.1017/S0266467405003007.

Jachmann, H., 2001. Estimating Abundance of African Wildlife: An Aid to Adaptive Management. Springer Science & Business Media.

Jachmann, H., 2002. Comparison of aerial counts with ground counts for large African herbivores. J. Appl. Ecol. 39 (5), 841–852.

Jetz, W., McGeoch, M.A., Guralnick, R., Ferrier, S., Beck, J., Costello, M.J., Fernandez, M., Geller, G.N., Keil, P., Merow, C., Meyer, C., Muller-Karger, F.E., Pereira, H.M., Regan, E.C., Schmeller, D.S., Turak, E., 2019. Essential biodiversity variables for mapping and monitoring species populations. Nat. Ecol. Evol. 3 (4) https://doi.org/10.1038/s41559-019-0826-1. Article 4.

Jolly, G.M., 1969. Sampling methods for aerial censuses of wildlife populations. East Afr. Agric. For. J. 34 (sup1), 46–49. https://doi.org/10.1080/00128325.1969.11662347.

Kellenberger, B., Marcos, D., Tuia, D., 2018. Detecting mammals in UAV images: best practices to address a substantially imbalanced dataset with deep learning. Remote Sens. Environ. 216, 139–153. https://doi.org/10.1016/j.rse.2018.06.028.

Lamprey, R., Ochanda, D., Brett, R., Tumwesigye, C., Douglas-Hamilton, I., 2020a. Cameras replace human observers in multi-species aerial counts in Murchison falls, Uganda. Remote Sens. Ecol. Conserv. 6 (4), 529–545. https://doi.org/10.1002/rse2.154.

Lamprey, R., Pope, F., Ngene, S., Norton-Griffiths, M., Frederick, H., Okita-Ouma, B., Douglas-Hamilton, I., 2020b. Comparing an automated high-definition oblique camera system to rear-seat-observers in a wildlife survey in Tsavo, Kenya: taking multi-species aerial counts to the next level. Biol. Conserv. 241, 108243 https://doi.org/10.1016/j.biocon.2019.108243.

Lamprey, R.H., Keigwin, M., Tumwesigye, C., 2023. A high-resolution aerial camera survey of Uganda's Queen Elizabeth Protected Area improves detection of wildlife and delivers a surprisingly high estimate of the elephant population (p. 2023.02.06.525067). bioRxiv. https://doi.org/10.1101/2023.02.06.525067.

LeCun, Y., Bengio, Y., Hinton, G., 2015. Deep learning. Nature 521 (7553). https://doi.org/10.1038/nature14539. Article 7553.

Lethbridge, M., Stead, M., Wells, C., 2019. Estimating kangaroo density by aerial survey: a comparison of thermal cameras with human observers. Wildl. Res. 46 (8), 639–648. https://doi.org/10.1071/WR18122.

Lisein, J., Linchant, J., Lejeune, P., Bouché, P., Vermeulen, C., 2013. Aerial surveys using an unmanned aerial system (UAS): comparison of different methods for estimating the surface area of sampling strips. Trop. Conserv. Sci. 6 (4), 506–520. https://doi.org/10.1177/194008291300600405.

Naudé, J., Joubert, D., 2019. The Aerial Elephant Dataset: A New Public Benchmark for Aerial Object Detection, pp. 48–55.

Norton-Griffiths, M., 1976. Further aspects of bias in aerial census of large mammals. J. Wildl. Manag. 40 (2), 368–371. https://doi.org/10.2307/3800445.

Norton-Griffiths, M., 1978. Counting Animals (J.J.R Grimsdell). African Wildlife Leadership Foundation.

PAEAS, 2014. Aerial Survey Standards and Guidelines for the Pan-African Elephant Aerial Survey. Vulcan Inc.

Peng, J., Wang, D., Liao, X., Shao, Q., Sun, Z., Yue, H., Ye, H., 2020. Wild animal survey using UAS imagery and deep learning: modified faster R-CNN for kiang detection in Tibetan Plateau. ISPRS J. Photogramm. Remote Sens. 169, 364–376. https://doi.org/10.1016/j.isprsjprs.2020.08.026.

Tkachenko, M., Malyuk, M., Holmanyuk, A., Liubimov, N., 2020. Label Studio: Data labeling software [Computer software]. https://github.com/heartexlabs/label-studio.

Tuia, D., Kellenberger, B., Beery, S., Costelloe, B.R., Zuffi, S., Risse, B., Mathis, A., Mathis, M.W., van Langevelde, F., Burghardt, T., Kays, R., Klinck, H., Wikelski, M., Couzin, I.D., van Horn, G., Crofoot, M.C., Stewart, C.V., Berger-Wolf, T., 2022. Perspectives in machine learning for wildlife conservation. Nat. Commun. 13 (1) https://doi.org/10.1038/s41467-022-27980-y. Article 1.

Wal, E.V., Mcloughlin, P.D., Brook, R.K., 2011. Spatial and temporal factors influencing sightability of elk. J. Wildl. Manag. 75 (6), 1521–1526.

World Wildlife Fund, 2007. Africa: River Network, 15s resolution, 2007—University of Texas Libraries GeoData [Map]. Geological Survey. https://geodata.lib.utexas.edu/catalog/stanford-wf122zm7811.